

A method for assessing metabolic information on liver and bone marrow by use of double gradient-echo with spectral fat suppression

メタデータ	言語: eng 出版者: 公開日: 2017-10-03 キーワード (Ja): キーワード (En): 作成者: メールアドレス: 所属:
URL	http://hdl.handle.net/2297/39852

Title:

A method for assessing metabolic information on liver and bone marrow by use of double gradient-echo with spectral fat suppression

Authors:

Harumasa Kasai, MS

Division of Health Sciences, Graduate School of Medical Science, Kanazawa University, 5-11-80, Kodatsuno, Kanazawa, Ishikawa 920-0942, Japan

Tel: +81-76-265-2540,

FAX: +81-76-234-4366

E-mail: hhkasai@gmail.com

Department of Central Radiology, Nagoya City University Hospital, 1 Kawasumi, Mizuho-cho, Mizuho-ku, Nagoya, 467-8602 Japan

Tosiaki Miyati, PhD, DMSc

Division of Health Sciences, Graduate School of Medical Science, Kanazawa University, 5-11-80, Kodatsuno, Kanazawa, Ishikawa 920-0942, Japan

Tel: +81-76-265-2540,

FAX: +81-76-234-4366

E-mail: ramiyati@mhs.mp.kanazawa-u.ac.jp

Tatsuya Kawai, MD

Department of Radiology, Nagoya City University Graduate School of Medical Sciences, 1 Kawasumi, Mizuho-cho, Mizuho-ku, Nagoya, 467-8601 Japan

E-mail: tatsuyakawai@gmail.com

Yuta Shibamoto, MD, DMSc

Department of Radiology, Nagoya City University Graduate School of Medical Sciences, 1 Kawasumi, Mizuho-cho, Mizuho-ku, Nagoya, 467-8601 Japan

E-mail: yshiba@med.nagoya-cu.ac.jp

Hirohito Kan, MS

Department of Central Radiology, Nagoya City University Hospital, 1 Kawasumi, Mizuho-cho, Mizuho-ku, Nagoya, 467-8602 Japan

E-mail: gpx246@yahoo.co.jp

Makoto Kawano, MS

Department of Central Radiology, Nagoya City University Hospital, 1 Kawasumi, Mizuho-cho, Mizuho-ku, Nagoya, 467-8602 Japan

E-mail: rakawano@med.nagoya-cu.ac.jp

A Method for Assessing Metabolic Information on Liver and Bone Marrow by Use of Double
Gradient-echo with Spectral Fat suppression

ABSTRACT

Our aim in this study was to create a noninvasive and practical method for evaluating metabolic information on the liver (iron content and lipid infiltration) and spine (bone mineral density and marrow fat degeneration) by using double gradient-echo with and without the spectral fat suppression technique (double-GRE-FS). We arranged phantoms made of various concentrations of superparamagnetic iron oxide solution adjacent to neutral fat to obtain slice planes with various fat fractions by using the partial volume effect. We obtained double-GRE-FS images and calculated the T_2^* values. The fat fraction was calculated from signal intensities of double-GRE-FS images after T_2^* decay, baseline, and slope corrections. We assessed the fat fraction and the relationship between R_2^* of the water component and the iron concentration. In addition, we evaluated those values in human bone marrow and liver, including a patient with liver steatosis. The actual fat fraction value was consistent with the fat fraction obtained with the double-GRE-FS method, and the calculated fat fraction was unaffected by the iron concentration. There was a strong positive correlation between R_2^* of the water component and the iron concentration. There was a negative correlation between the fat fraction and the bone mineral density, and the R_2^* was correlated with the bone mineral density. The calculated fat fraction in the liver steatosis patient was significantly higher than that in healthy volunteers. The double-GRE-FS makes it possible to assess the fat fraction and R_2^* simultaneously, and to obtain metabolic information on the liver and bone marrow.

Keywords: MRI, fat fraction, relaxation rate, liver, bone marrow

1 Introduction

Metabolic information on the liver and bone marrow has been evaluated by use of magnetic resonance imaging (MRI) [1-4]. Two kinds of quantitative analytical methods, i.e., fat fraction and transverse relaxation rate (R_2^*) analyses, were applied for assessment of the liver and bone marrow with MRI. The fat fraction analyses were applied for the diagnosis of fatty liver (or nonalcoholic steatohepatitis) [5, 6] and osteoporosis [7]. The R_2^* analyses were applied for the evaluation of diseases with iron overload such as hemosiderosis and hemochromatosis [8] and for bone mineral density (BMD) [6].

In recent studies, several methods for simultaneously determining the fat fraction and R_2^* have been developed by Wehrli et al. [7], Yu et al. [8], Matsunaga et al. [9], and Motono et al. [10], and both fat content and R_2^* analyses were performed at one time. However, these methods require a special sequence and an analysis program.

Our aim in this study was to create a noninvasive and practical method for evaluating metabolic information on the liver (iron content and lipid infiltration) and spine (bone mineral density and marrow fat degeneration) by using double gradient-echo (GRE) with and without the spectral fat suppression technique (double-GRE-FS). To address this issue, we conducted a phantom study and then applied it to clinical cases.

2 Materials and Methods

Procedure for Fat Content and R_2^ Analyses*

The procedure for obtaining the fat content and R_2^* by using double-GRE-FS is shown in Fig. 1. On a 1.5-T MRI, we obtained sagittal (for spine) or transverse (for liver) double-GRE images (the in-phase first echo time [TE_1] and second echo time [TE_2] were 4.6 msec and 9.2 msec, respectively) with and without spectral attenuated inversion recovery (SPAIR). We then placed regions of interest (ROI) in the bone (spine) or liver (Fig. 2), and we determined each mean signal intensity. In the healthy liver, the ROI was positioned away from large vessels, and the size of the ROI was unified by approximately 475 to 540 mm². In liver steatosis, the ROI was positioned in hyperechogenicity of the liver relative to the kidney on ultrasonography (US) away from large vessels. In the spine, the ROIs covered the entire bone marrow of

each vertebra. One vertebral body was covered by one ROI measurement. Moreover, we measured signal intensities in the subcutaneous fat area and in the non-pulsatile cerebrospinal flow (CSF) space as internal references (Fig. 2).

To determine the fat fraction, we first corrected the T_2^* decay and obtained the initial signal intensities (I_0 at $TE = 0$) as follows:

$$I_0 = I_1 / \exp\{-TE_1 \ln(I_1 / I_2) / (TE_2 - TE_1)\} = I_1 (I_1 / I_2)^{TE_1 / (TE_2 - TE_1)}.$$

Because TE_2 was set at $2TE_1$,

$$I_0 = I_1^2 / I_2,$$

where I_1 and I_2 are the signal intensities at TE_1 and TE_2 with and without SPAIR images, respectively.

Next, we calculated the provisional fat fraction (FF_{prov}) according to the following equation:

$$FF_{prov} (\%) = 100 (I_{0-off} - I_{0-on}) / I_{0-off},$$

where I_{0-off} is the initial signal intensity without SPAIR, and I_{0-on} is that with SPAIR. We also calculated a fat fraction value in the non-pulsatile CSF space (FF_w), and we then corrected the baseline to make the fat content of the 100%-water area zero by using the following equation (Fig. 1a):

$$FF_{bc} (\%) = FF_{prov} - FF_w$$

Finally, we calculated another fat fraction value in the subcutaneous fat area (FF_f), and we corrected the slope between the MR-derived fat fraction and the actual fat fraction as follows (Fig. 1b):

$$FF (\%) = 100 FF_{bc} / FF_f,$$

where we assume that the fat fraction of the subcutaneous fat is nearly 100 percent.

In addition, we measured the R_2^* values of the water component of the bone or liver obtained from the double-GRE images with SPAIR, using the following equation:

$$R_2^* = \ln(I_1/I_2) / (TE_2 - TE_1).$$

MRI System and Acquisition Protocols

On a 1.5T-MRI (Gyrosan Intera, Philips Medical Systems, BEST, the Netherlands), the double-GRE-FS was used with a 4-channel body coil. The first in-phase echo (TE_1) and second in-phase echo (TE_2) of the double-GRE were 4.6 and 9.2 ms, respectively. The repetition time (TR) was set at 240 ms, and the flip angle was 12 degrees to minimize the T_1 effect. The double-GRE sequence with SPAIR (TI = 80 ms) was

set with the same conditions. The acquisition time of each sequence was from 16 to 123 seconds.

Phantom Study

Iron solution with various concentrations (0, 0.05, 0.20, 0.60 and 1.00 mmol/L) of superparamagnetic iron oxide (SPIO) and neutral fat were arranged together in plastic bottles. As shown in Fig. 3, the neutral fat and SPIO solution were separated into upper and lower layers. This phantom was scanned with the double-GRE-FS, and various images with different fat contents (0, 10, 20, 30, 40, 60, 90 and 100%) were obtained by shifting of the slice planes upward or downward at the interface of the iron solution and neutral fat by use of the partial volume effect. It was assumed that 100%-fat and 100%-water components were equivalent to the subcutaneous fat and CSF in the human body, respectively. The scan parameters were set at 200 x 200 mm field of view (FOV), 40 mm slice thickness, 256 x 256 acquisition matrix, and the two signals averaged in addition to the above-mentioned acquisition protocols.

We evaluated the relationship between the R_2^* of the water component and the iron concentration, the relationship between the fat fraction value calculated by our method (Fig. 1) and actual fat fractions, and the influence of the iron concentration on the fat fraction.

Preliminary Clinical Study

Approval for the clinical study was obtained from our institutional review board. Written informed consent was obtained from all subjects, and the liver and the lumbar spine were evaluated (see “procedure for fat content and R_2^* analyses”) (Figs. 1 and 2). Concerning the double-GRE-FS imaging conditions, the TR, TE, and flip angle were set at the same conditions used in the phantom study. The other scan parameters were set at 300 x 300 mm FOV, 8 mm slice thickness, and 192 x 192 acquisition matrix. Rectangular FOV and sensitivity encoding techniques were used for the liver breath–hold imaging.

Regarding the liver analysis, subjects consisted of five healthy volunteers (controls) and five patients with fatty livers, defined as having hyperechogenicity (ROI in double-GRE-FS images) of the liver relative to the kidney on US. The liver fat fraction and R_2^* were determined in each group, and the influence of the fat fraction on R_2^* was assessed. For the lumbar spine (L3 - L5), subjects consisted of five healthy male volunteers, and their bone mineral densities had been obtained previously by use of

dual-energy X-ray absorptiometry (DXA-BMD).

All statistical analyses were performed by use of software (SPSS for Windows, version 18.0; SPSS, Chicago, IL). We used the Mann-Whitney U test and the Wilcoxon signed-rank test to determine the significance between control and liver steatosis groups, and pre- and post-corrections of the fat fraction, respectively. The relationships between measurement values were assessed by multiple linear regression analysis. $P < .05$ was considered to indicate a significant difference.

3 Results

In the phantom study, there was a strong positive correlation between R_2^* calculated from the water component obtained with double-GRE-FS and the iron concentration ($R^2 = 0.941, 0.941, 0.923, 0.907$ at fat contents of 10, 20, 30 and 40%, respectively)(Fig. 4). Figure 5 shows the effects of correction procedures for double-GRE-FS. After T_2^* correction (Fig. 5b) and after the baseline and slope corrections of fat content (Fig. 5c), the fat content was consistent with the actual value, and the linearity between them at each iron concentration was improved compared to the values before corrections (after corrections, mean $R^2 = 0.996 \pm 0.002$, mean slope = 0.990 ± 0.008 , and mean ordinate intercept = $0.27 \pm 2.10\%$; before corrections, mean $R^2 = 0.989 \pm 0.005$, mean slope = 0.676 ± 0.135 , and mean ordinate intercept = $23.90 \pm 14.49\%$).

Fat fractions of the liver and the lumbar spine from a preliminary clinical study by use of double-GRE-FS are shown in Fig. 6. Significant differences were found between the fat content values before and after corrections in all groups. The mean fat content of the fatty liver was significantly higher than that of the controls (fatty liver, $14.4 \pm 4.9\%$; controls, $6.4 \pm 1.3\%$; $P = 0.009$) (Fig. 6). The double-GRE-FS method could obtain R_2^* of the liver water component independent of the liver fat content (Fig. 7). In the lumbar spine (mean values on L3 - L5), there tended to be a positive correlation between R_2^* of the water component and DXA-BMD ($R^2 = 0.733$) (Fig 8a), and there was a negative correlation between DXA-BMD and fat content by use of double-GRE-FS ($R^2 = 0.913$) (Fig. 8b).

4 Discussion

Fat fraction analyses were useful for assessment of regional fatty degeneration/lipid infiltration, i.e., fatty liver, nonalcoholic steatohepatitis [5, 6], osteoporosis [7], radiation-induced fatty degeneration of the bone marrow [11], aplastic anemia, and bone aging [10]. R_2^* analyses were applied for the evaluation of osteoporosis [7] and of diseases with iron overload such as hemochromatosis and hemosiderosis [8]. Previously, simultaneous analyses of the fat fraction and R_2^* were difficult, and some researchers performed simultaneous analyses of both fat content and R_2^* [7-10]. However, those analytic methods require a special pulse sequence and a complicated algorithm, which are usually absent in clinical MRI. Therefore, we performed double-GRE with the spectral fat suppression method that is available in the general MRI system, and the fat fraction and R_2^* were analyzed simultaneously.

In the phantom study, there was a linear correlation between the iron concentration and R_2^* of the water component obtained by use of double-GRE-FS method even fat-containing regions (Fig. 4). This meant that the iron concentration can be evaluated by determination of the R_2^* of the water component, independent of the liver fat content (Fig. 7). Spectral fat suppression techniques such as SPAIR cannot completely suppress the fat signal [12, 13]. Moreover, the signal intensity of the 100%-water area with SPAIR is not always equal to that without SPAIR, because this depends on the receiver gain and the cross talk between fat and water spectra due to field inhomogeneity. We therefore applied baseline and slope corrections of the fat content to the double-GRE-FS analysis by using an internal reference, i.e., 100%-water and 100%-fat regions, in addition to the T_2^* correction. In fact, the fat content obtained with double-GRE-FS coincided well with the actual value after these corrections (Fig. 5b), indicating that there is a need for corrections.

In preliminary clinical studies, significant differences were found between the fat content values with double-GRE-FS before and after the correction processes for all groups of our method. Fat fraction values calculated with this method showed a higher value in the fatty-liver group than that in the control group, suggesting the clinical usefulness of the method (Fig. 6). Furthermore, there was no significant correlation between R_2^* of the water component and the fat content in the liver, meaning that assessment of the iron concentration in the liver was unaffected by fat content (Fig. 7). Thus, this method might be useful for assessing both the fat content and the iron concentration in a fatty liver with hemosiderosis and

hemochromatosis ($R_2^* = 187 \text{ s}^{-1}$ [8]) [6], or after the injection of SPIO [14]. In the lumbar spine, a positive correlation between R_2^* of the water component and BMD, and a negative correlation between the fat fraction and BMD (Fig. 8), indicated that the amount of information on bone and marrow metabolism might be increased by use of this method [7, 10].

The double-GRE-FS method enables us to obtain the fat fraction and the R_2^* easily by measuring the same slice plane twice, with and without spectral fat suppression. Because SPAIR as a spectral fat suppression technique used the adiabatic pulse which is relatively insensitive to B_1 variations [14, 15], it has wide clinical applications, including that to high-field MRI systems. On the other hand, our study has several limitations. First, olefinic protons close to the water peak are unsaturated lipids even if the spectral fat suppression technique is used [13]. However, only the signals from methylene and methyl protons were of clinical significance, especially in hepatic steatosis [16], and the small contribution of olefinic protons of lipids to the water peak was neglected [17]. Second, to correct the fat fraction, we assumed that the fat fraction of the subcutaneous fat, i.e., almost white adipose tissue in the human adult, was nearly 100 percent, and we then measured the subcutaneous fat signal as an internal reference. However, since brown fat has considerable water content [18], other than subcutaneous fat, particularly in infants, should not be used as an internal reference. Third, since our patient populations were small, a further evaluation should be undertaken with a larger sample size to confirm the efficacy of the method described here. Despite these limitations, however, the double-GRE-FS, by use of a universal fat suppression technique without special equipment or application, makes simultaneous measurement of the metabolic information on the liver and bone marrow much easier.

5 Conclusion

We devised a noninvasive and practical method for evaluating metabolic information on the liver and spine, and we conducted a phantom study; then we applied the method to clinical cases. The double-GRE-FS makes it possible to assess the fat fraction and R_2^* simultaneously, and to obtain metabolic information on the liver (lipid infiltration and iron content) and bone marrow (bone mineral density and marrow fat degeneration).

Conflict of interest

The authors declare that they have no conflict of interest.

References

1. Bernard CP, Liney GP, Manton DJ, et al. Comparison of fat quantification methods: a phantom study at 3.0T. *J Magn Reson Imaging* 2008; 27:192-197.
2. Cotler SJ, Guzman G, Layden-Almer J, et al. Measurement of liver fat content using selective saturation at 3.0 T. *J Magn Reson Imaging* 2007; 25:743-748.
3. Alexopoulou E, Stripeli F, Baras P, et al. R2 relaxometry with MRI for the quantification of tissue iron overload in beta-thalassemic patients. *J Magn Reson Imaging* 2006; 23:163-170.
4. Storey P, Thompson AA, Carqueville CL, et al. R2* imaging of transfusional iron burden at 3T and comparison with 1.5T. *J Magn Reson Imaging* 2007; 25:540-547.
5. Hussain HK, Chenevert TL, Londy FJ, et al. Hepatic fat fraction: MR imaging for quantitative measurement and display--early experience. *Radiology* 2005; 237:1048-1055.
6. Mitsuyoshi H, Yasui K, Harano Y, et al. Analysis of hepatic genes involved in the metabolism of fatty acids and iron in nonalcoholic fatty liver disease. *Hepatol Res* 2009; 39:366-373.
7. Wehrli FW, Hopkins JA, Hwang SN, et al. Cross-sectional study of osteopenia with quantitative MR imaging and bone densitometry. *Radiology* 2000; 217:527-538.
8. Yu H, McKenzie CA, Shimakawa A, et al. Multiecho reconstruction for simultaneous water-fat decomposition and T₂* estimation. *J Magn Reson Imaging* 2007; 26:1153-1161
9. Matsunaga S, Miyati T, Onoguchi M, et al. Simple and accurate method for liver fat content analysis with dual double-gradient-echo MRI. *Medical Imaging and Information Sciences* 2006; 23:8-10..
10. Motono Y, Miyati T, Ueda Y, et al. Simultaneous analysis of marrow fat fraction and bone mineral density with modulus and real multiple gradient-echo MRI. *Medical Imaging and Information Sciences* 2010; 27:14-17.
11. Huang W, Yang Y, Sun Z, et al. Early radiation-induced bone marrow injury: serial MR imaging during initial 4 weeks after irradiation. *Acad Radiol* 2009; 16:733-738.
12. Tomita K, Tanimoto A, Irie R, et al. Evaluating the severity of nonalcoholic steatohepatitis with superparamagnetic iron oxide-enhanced magnetic resonance imaging. *J Magn Reson Imaging*

2008; 28:1444-1450.

13. Reeder SB, Pineda AR, Wen Z, et al. Iterative decomposition of water and fat with echo asymmetry and least-squares estimation (IDEAL): application with fast spin-echo imaging. *Magn Reson Med* 2005; 54:636-644.
14. Bley TA, Wieben O, Francois CJ, et al. Fat and water magnetic resonance imaging. *J Magn Reson Imaging* 2010; 31:4-18.
15. Rosenfeld D, Panfil SL, Zur Y. Design of adiabatic pulses for fat-suppression using analytic solutions of the Bloch equation. *Magn Reson Med* 1997; 37:793-801.
16. Liu CY, McKenzie CA, Yu H, et al. Fat quantification with IDEAL gradient echo imaging: correction of bias from T_1 and noise. *Magn Reson Med* 2007; 58:354-356.
17. Kugel H, Jung C, Schulte O, et al. Age- and sex-specific differences in the ^1H -spectrum of vertebral bone marrow. *J Magn Reson Imaging* 2001; 13:263-268.
18. Hu HH, Tovar JP, Pavlova Z, et al. Unequivocal identification of brown adipose tissue in a human infant. *J Magn Reson Imaging* 2012; 35:938-942.

Figure legends:

Figure. 1

Procedure for analyzing fat fraction (FF) and R_2^* of the spine or liver using the double-GRE-FS. a) Baseline and b) slope correction for making the MRI-derived fat content of 100%-water = 0% and of 100%-fat = 100%. CSF: cerebrospinal fluid. FF_{prov} : provisional fat fraction. FF_{bc} : fat fraction after baseline correction. BMD: bone mineral density.

Figure. 2

Double gradient-echo (GRE) images of the spine a) with and b) without spectral attenuated inversion recovery (SPAIR) in each echo time (TE), and liver double-GRE images c) with and d) without SPAIR. Mean signal intensities were determined in each region of interest. CSF: cerebrospinal fluid.

Figure. 3

Schema of the phantom model. Superparamagnetic iron oxide (SPIO) solution with various concentrations of iron [(a) 0, (b) 0.05, (c) 0.20, (d) 0.60 and (e) 1.00 mM] and neutral fat were arranged together in plastic bottles to produce phantom models. Neutral fat and SPIO solution were separated as upper and lower layers, respectively. (f) Only fat component without water section. (g) Only water component without fat section.

Figure. 4

Relationship between R_2^* of the water component obtained with double-GRE-FS and iron concentration in each fat fraction image of the phantom. The R_2^* was proportional to the iron concentration and was not affected by fat content.

Figure. 5

Relationship between fat fraction calculated from double-GRE-FS and actual fat content of the phantom at each iron concentration. (a) Before any correction procedures for fat content. (b) After T_2^* correction, and (c) after the baseline and slope corrections of fat content.

Figure. 6

Box plot of fat fraction data obtained from double-GRE-FS of the liver (control and steatosis) and the lumbar spine. The horizontal line is the median, the ends of the box are the upper and lower quartiles, and the vertical lines are the full range of values in the data. Pre: before corrections of the fat content. Post: after corrections.

Figure. 7

Relationship between R_2^* of the liver water component with use of double-GRE-FS and the liver fat fraction. Note that there was no significant correlation between them.

Figure. 8

Relationship between a) R_2^* of the water component or b) fat fraction with use of double-GRE-FS and the bone mineral density with use of dual-energy X-ray absorptiometry (DXA-BMD) in the lumbar spine.

1. Scan using double gradient-echo with and without spectral presaturation with inversion recovery (SPAIR); double-GRE-FS

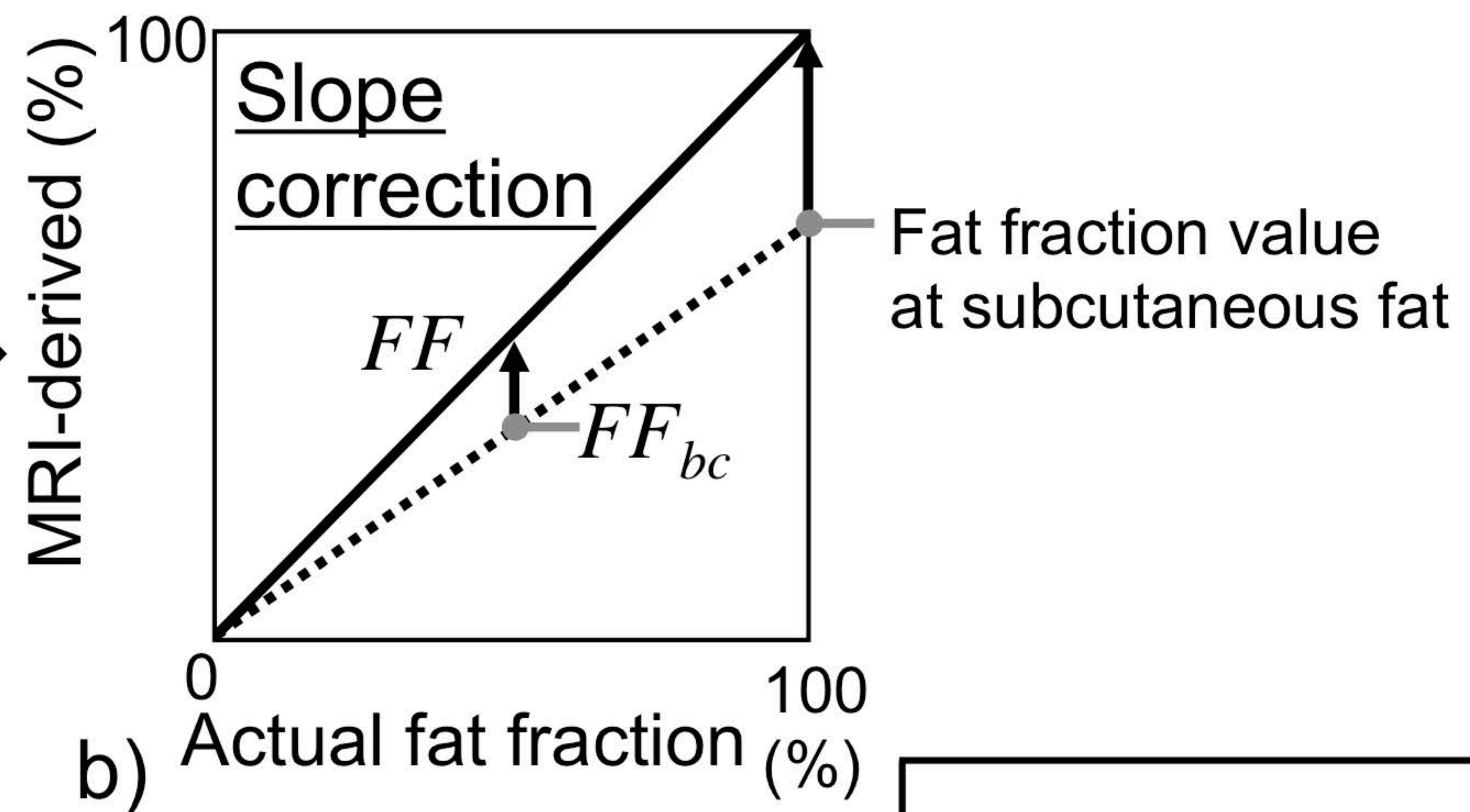
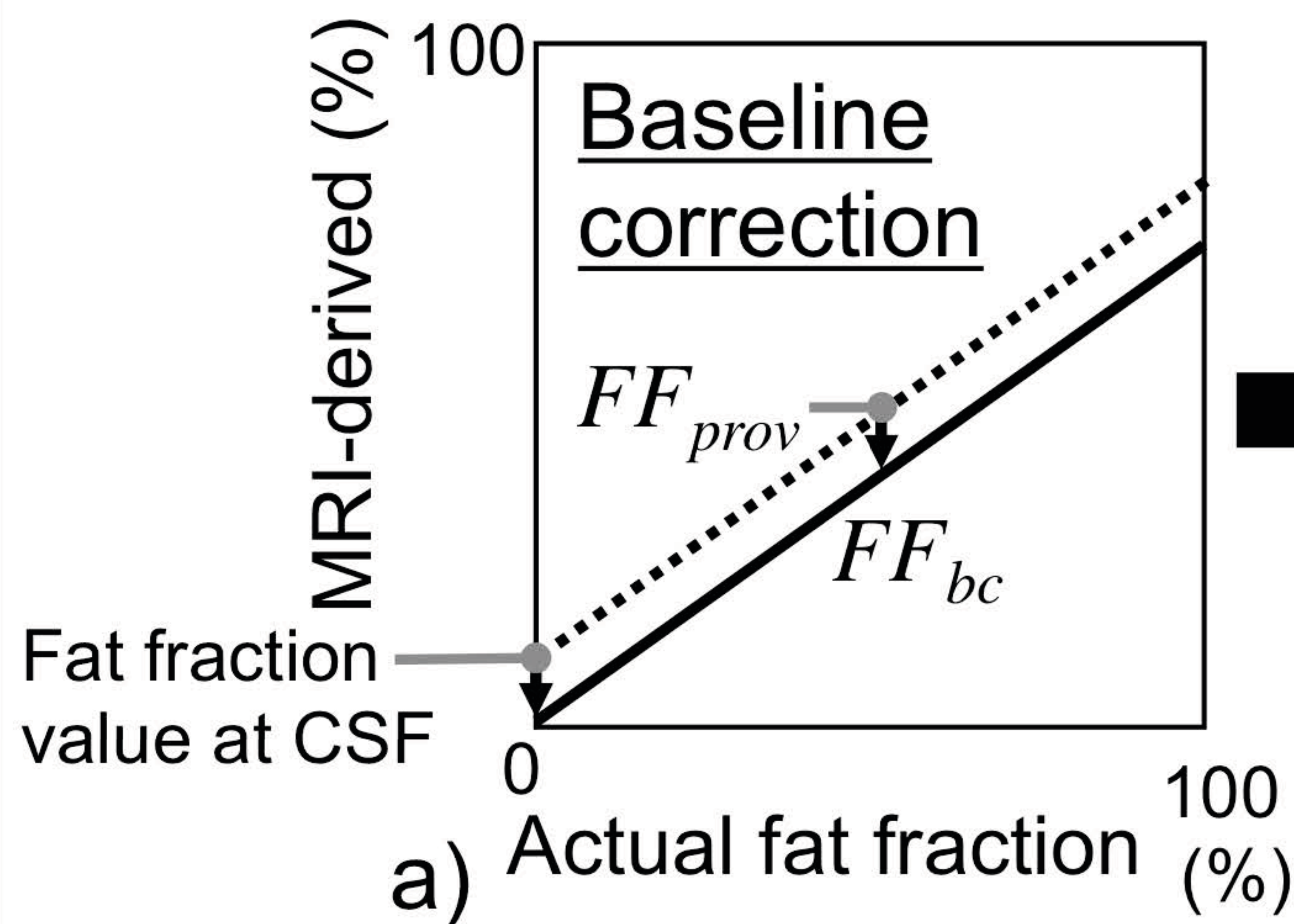
2. Signal intensity measurements of the liver or bone, CSF, and subcutaneous fat

[see Fig. 2]

3. Correction of T_2^* decay

5. R_2^* analysis of SPAIR_{on} image

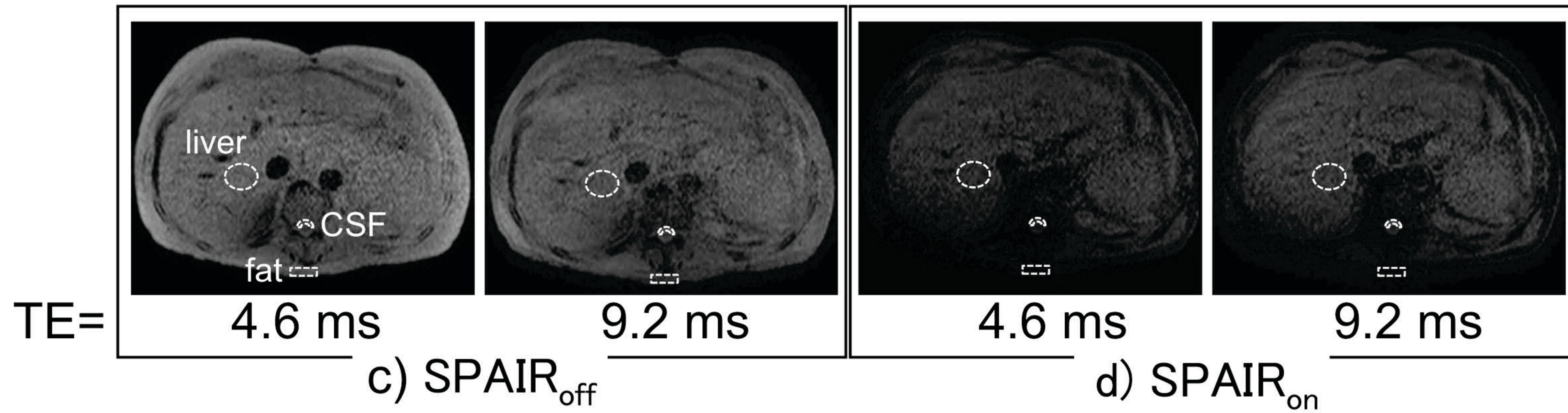
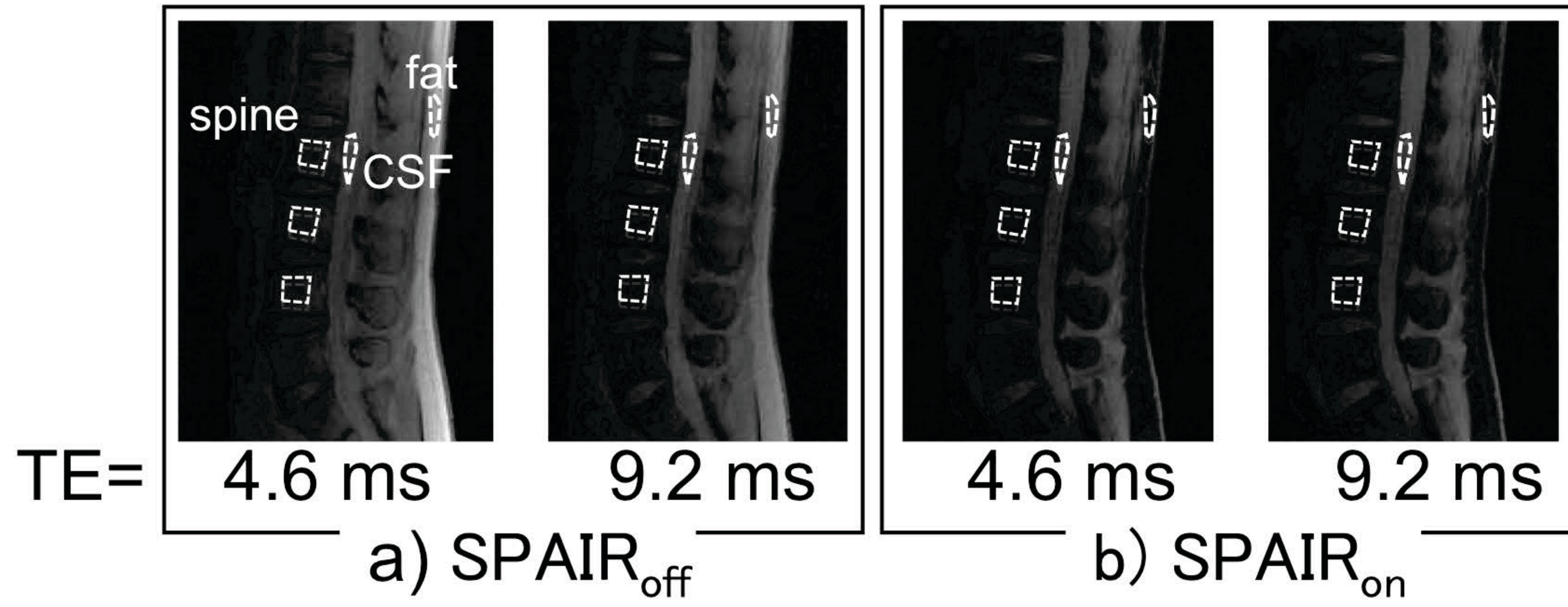
4. Fat fraction (FF) analysis with baseline and slope corrections

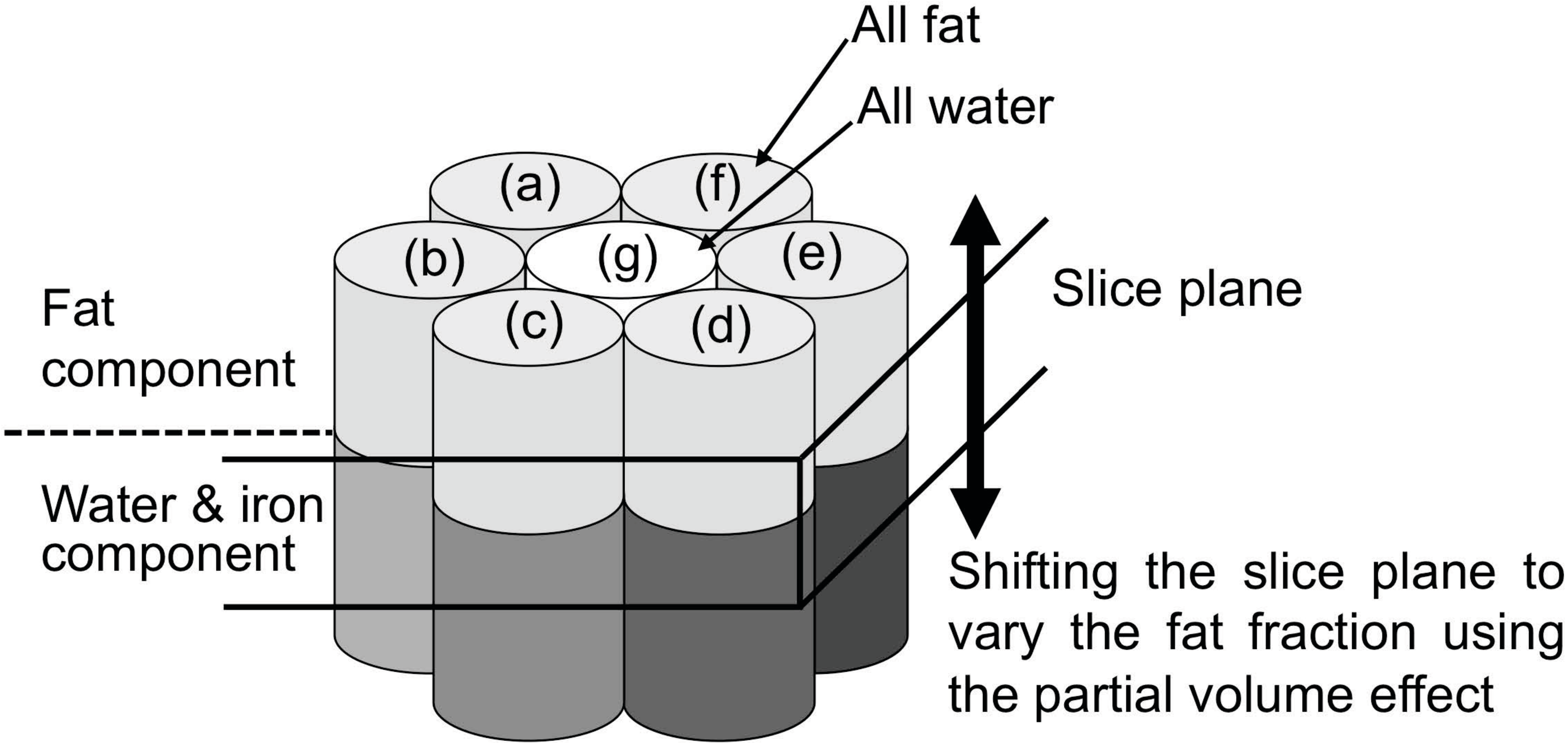


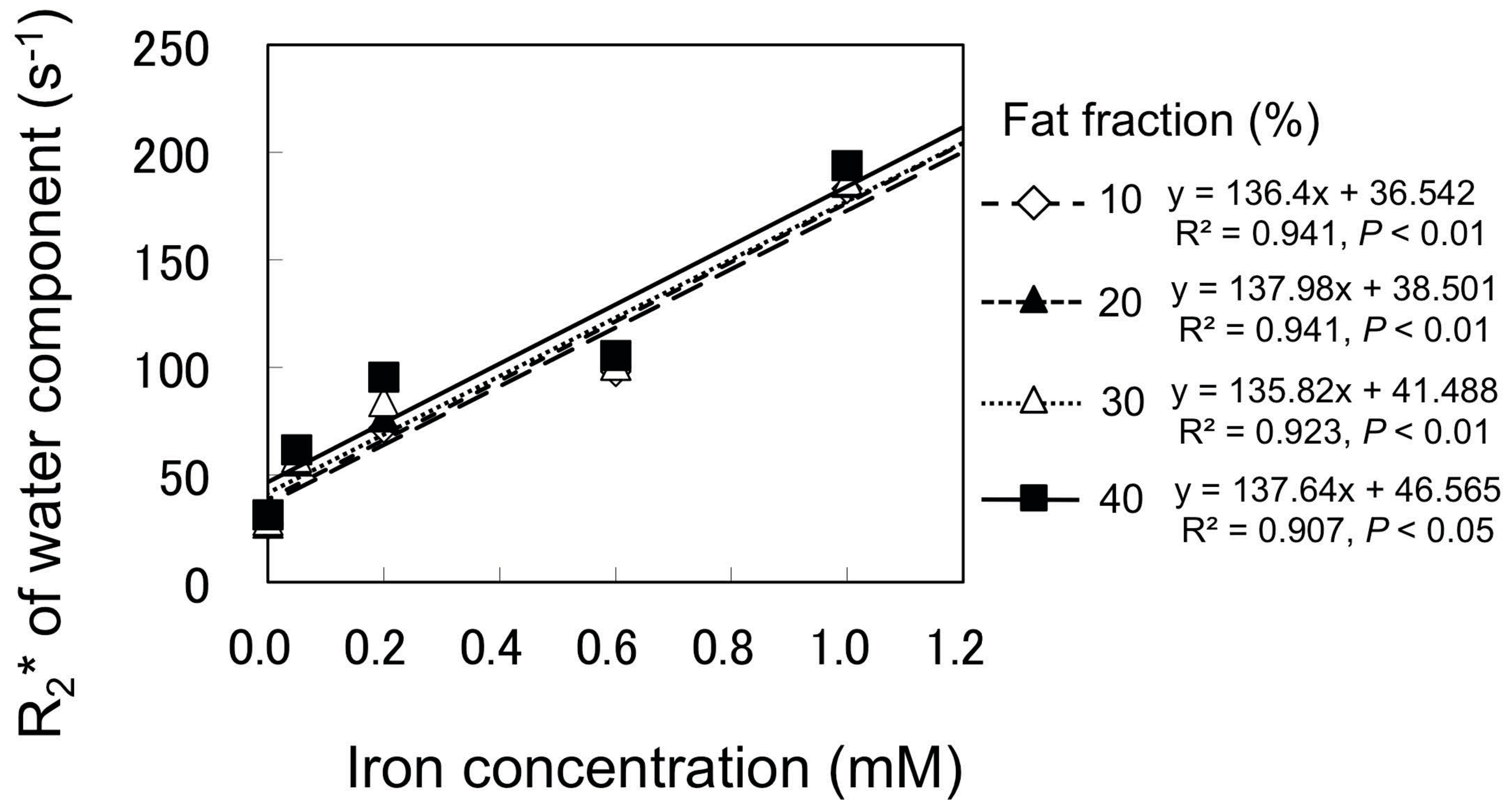
FF of the liver or bone marrow

Bone: BMD

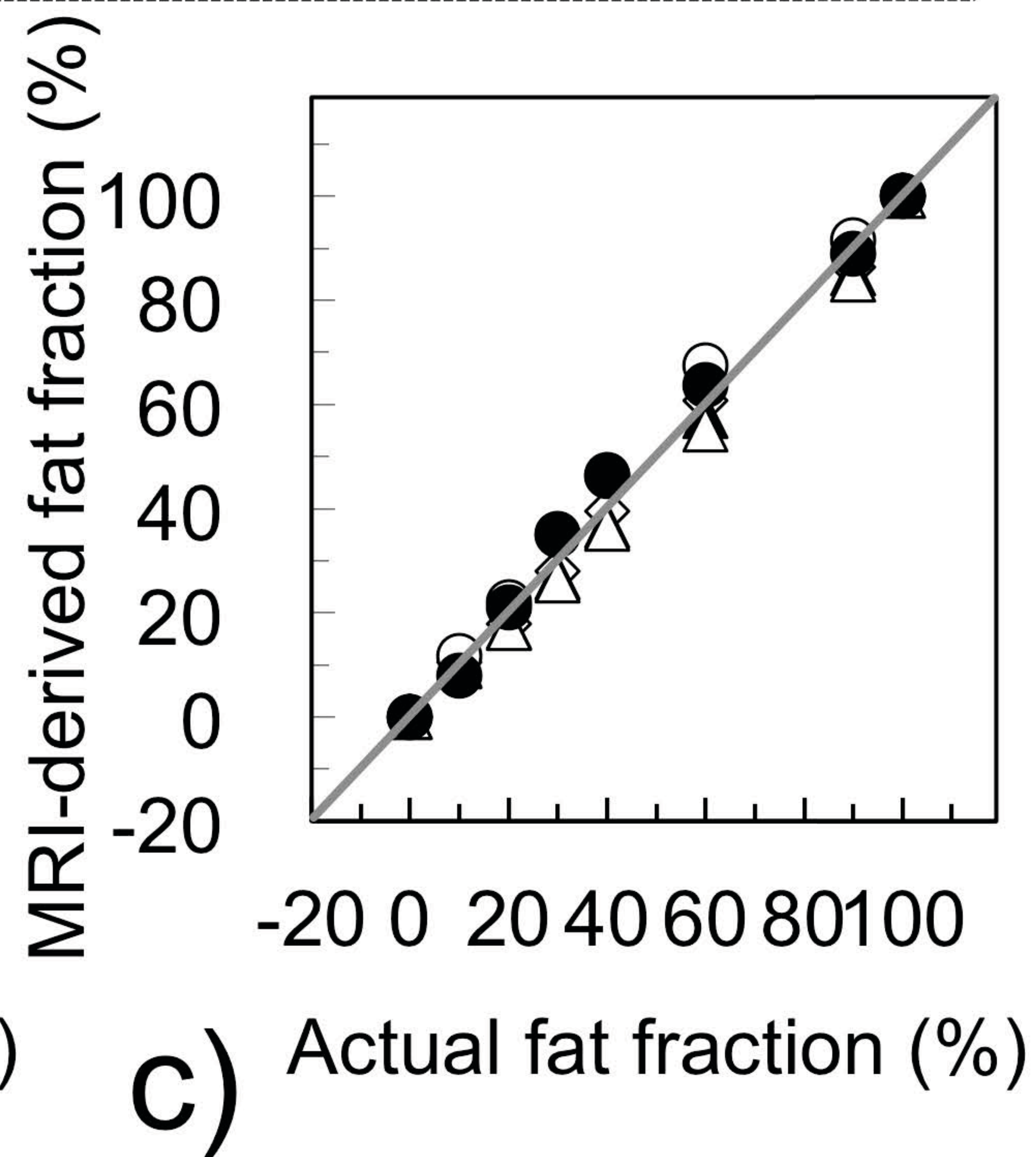
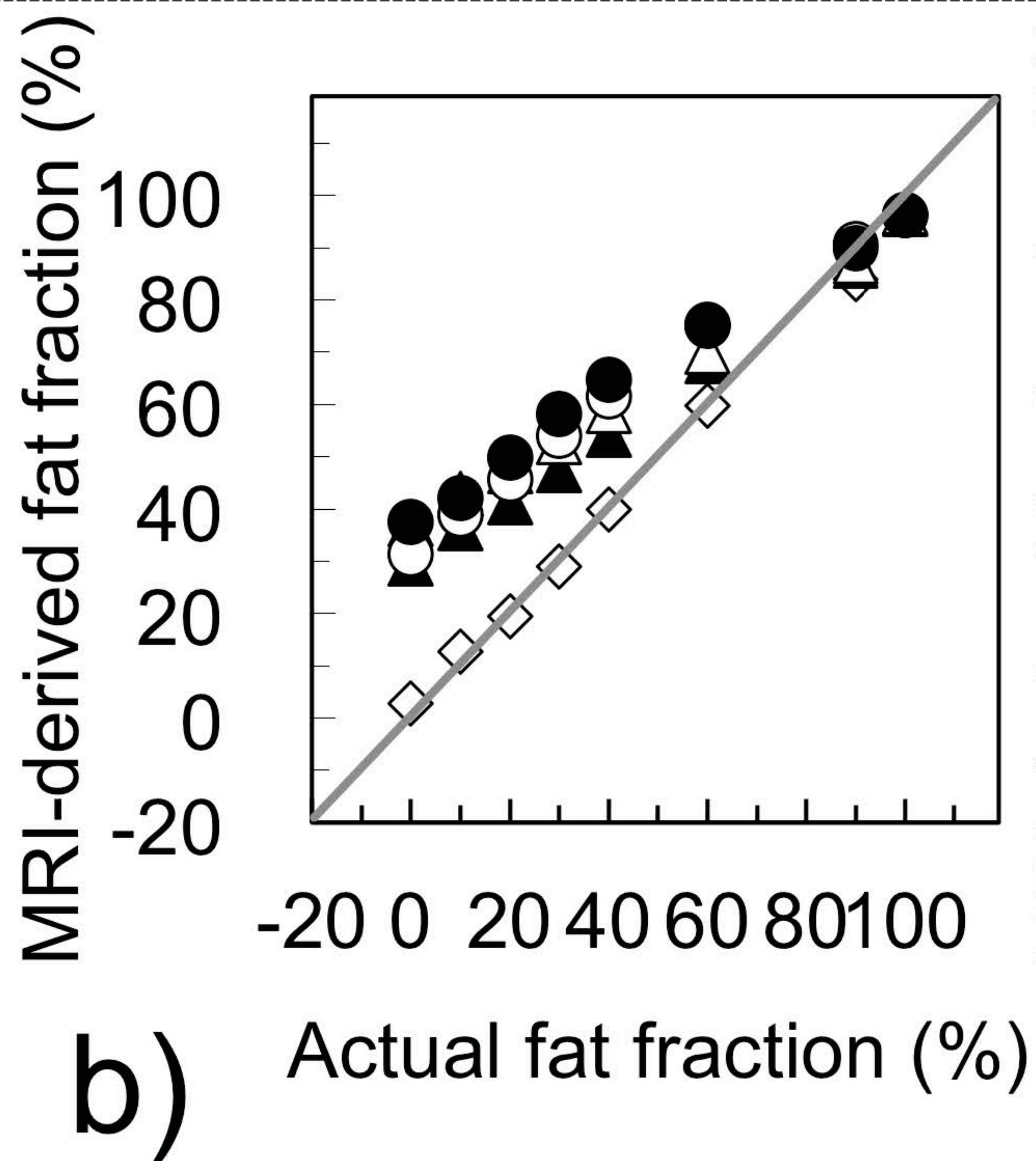
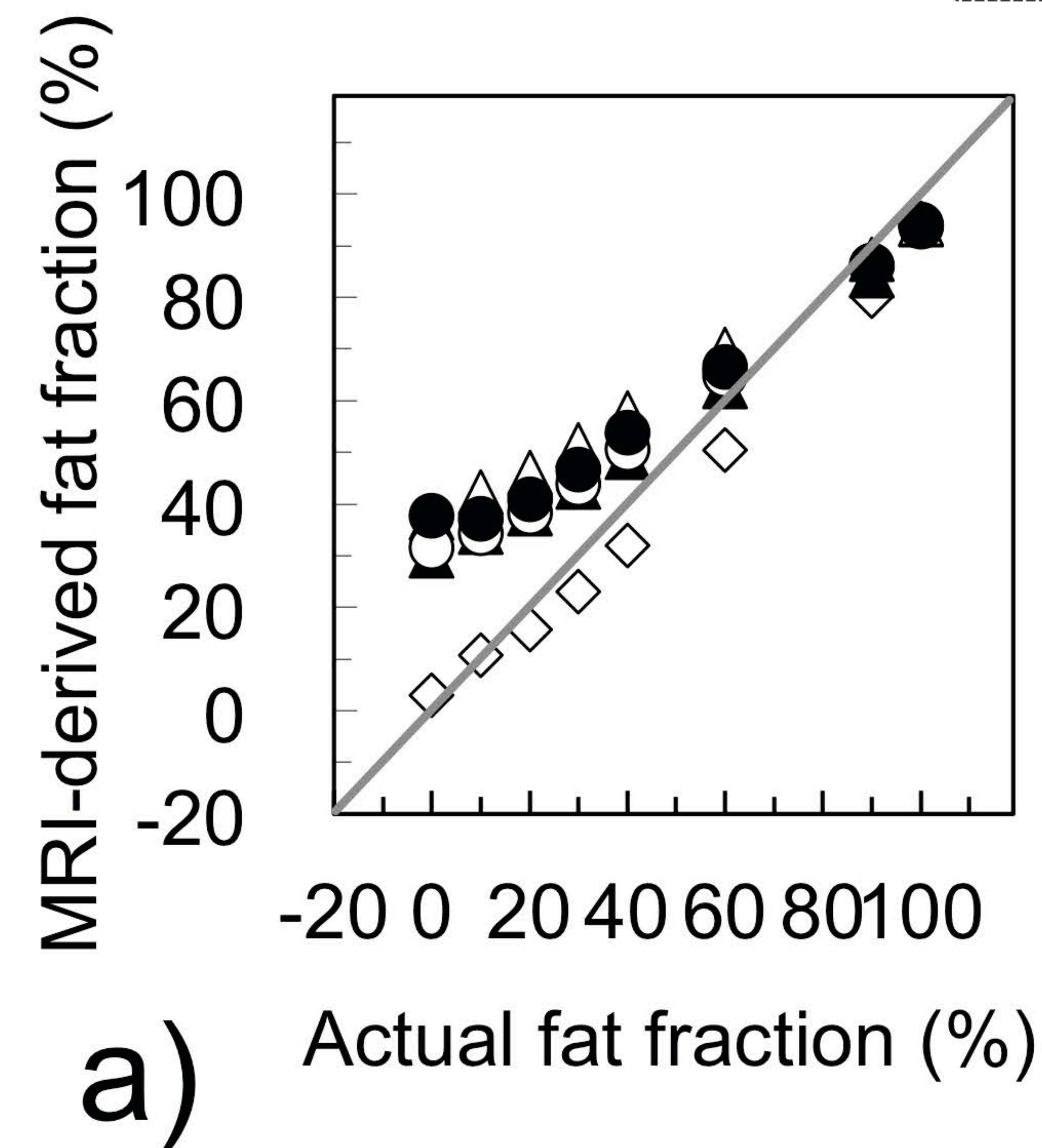
Liver: iron content

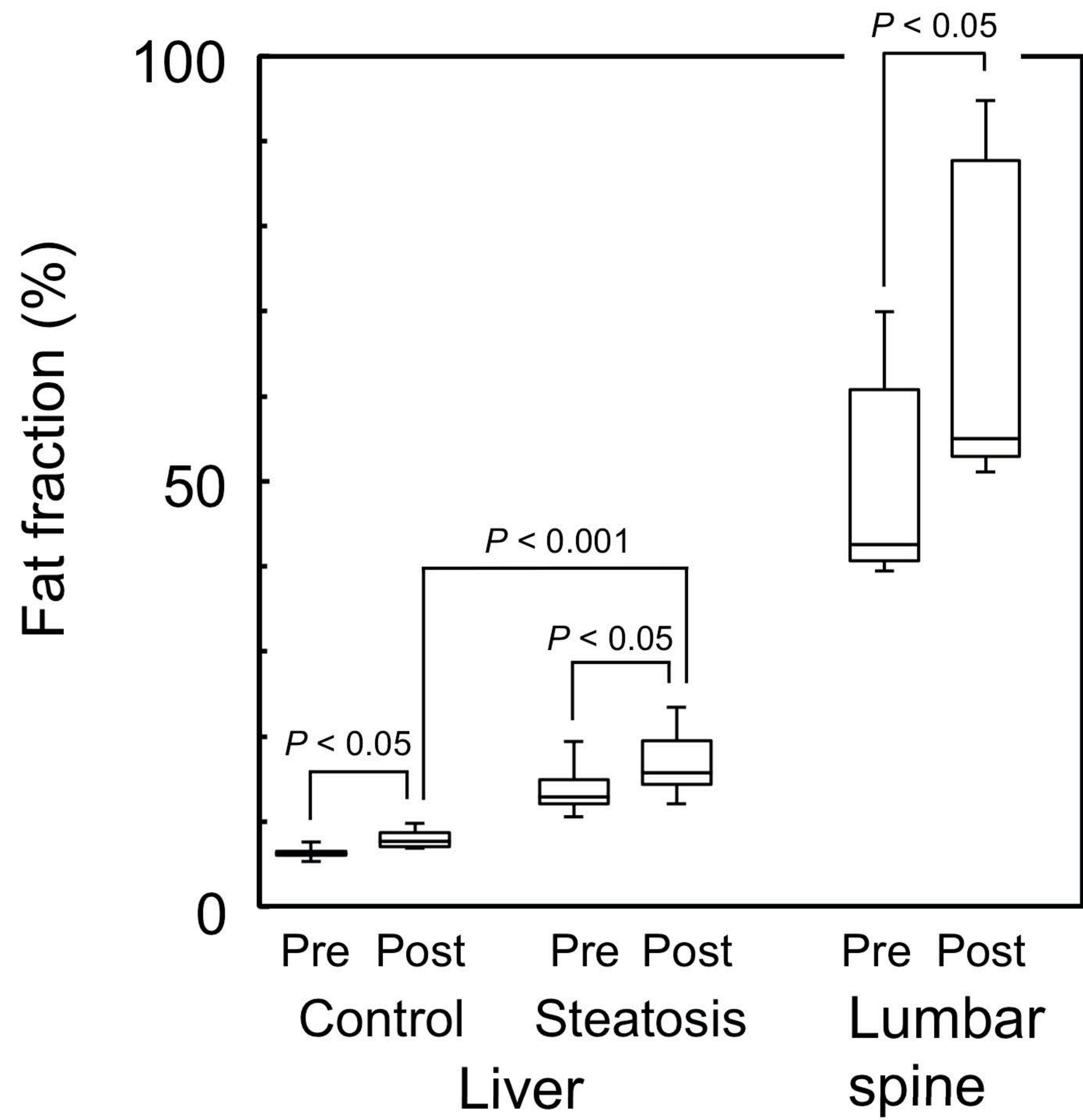


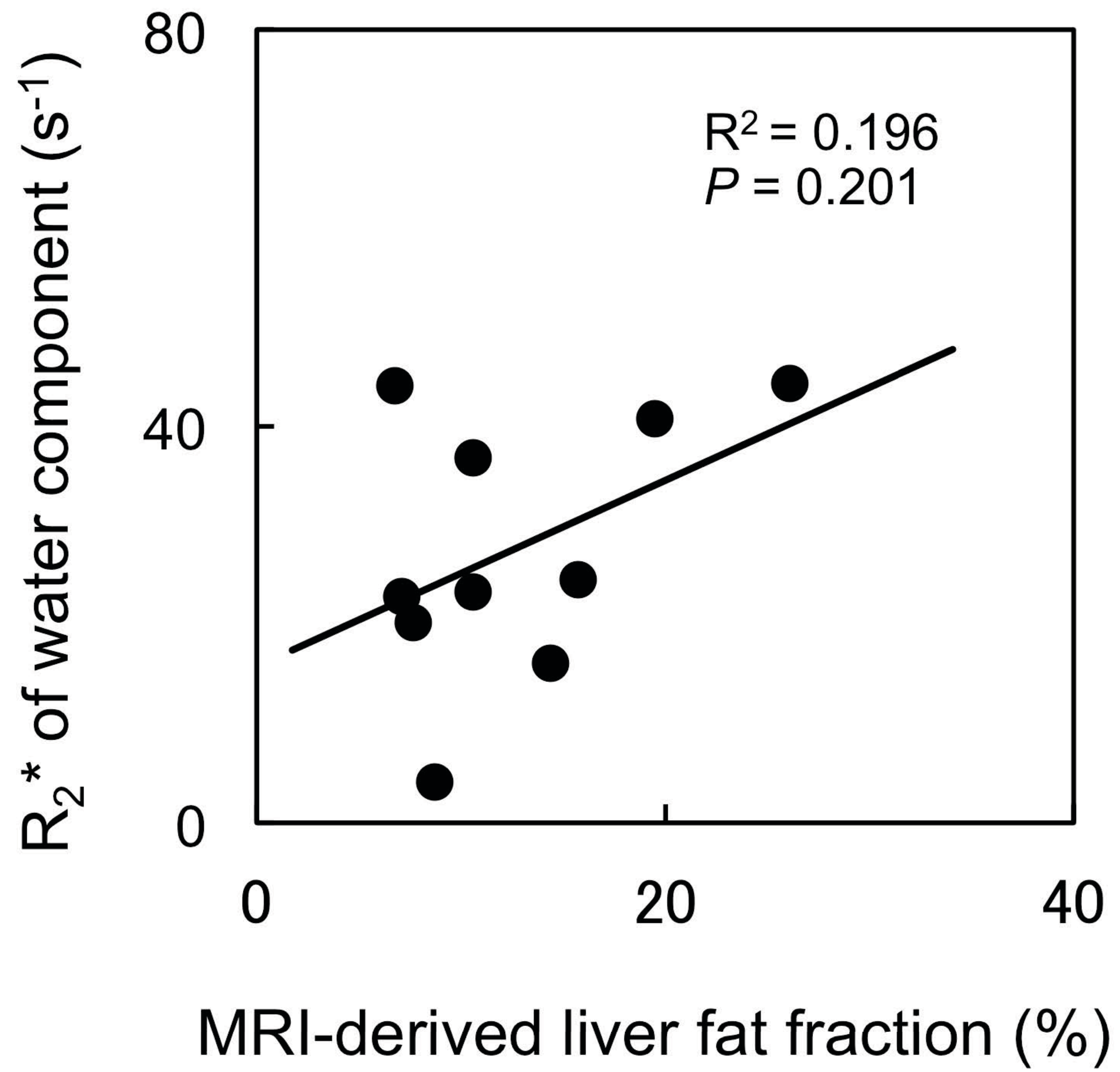




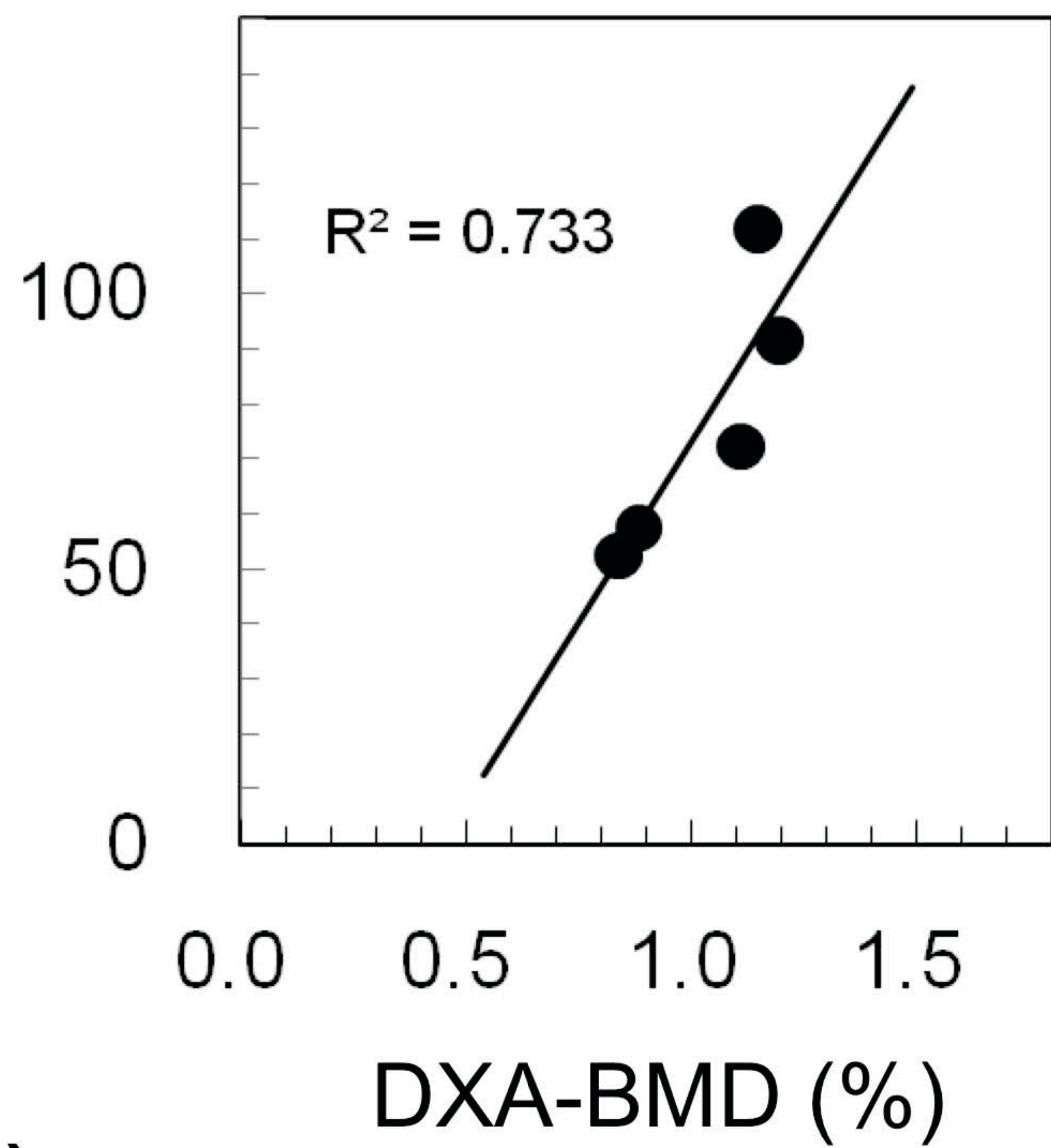
Iron concentration (mM) \diamond 0.00 \blacktriangle 0.05 \triangle 0.20 \circ 0.60 \bullet 1.00





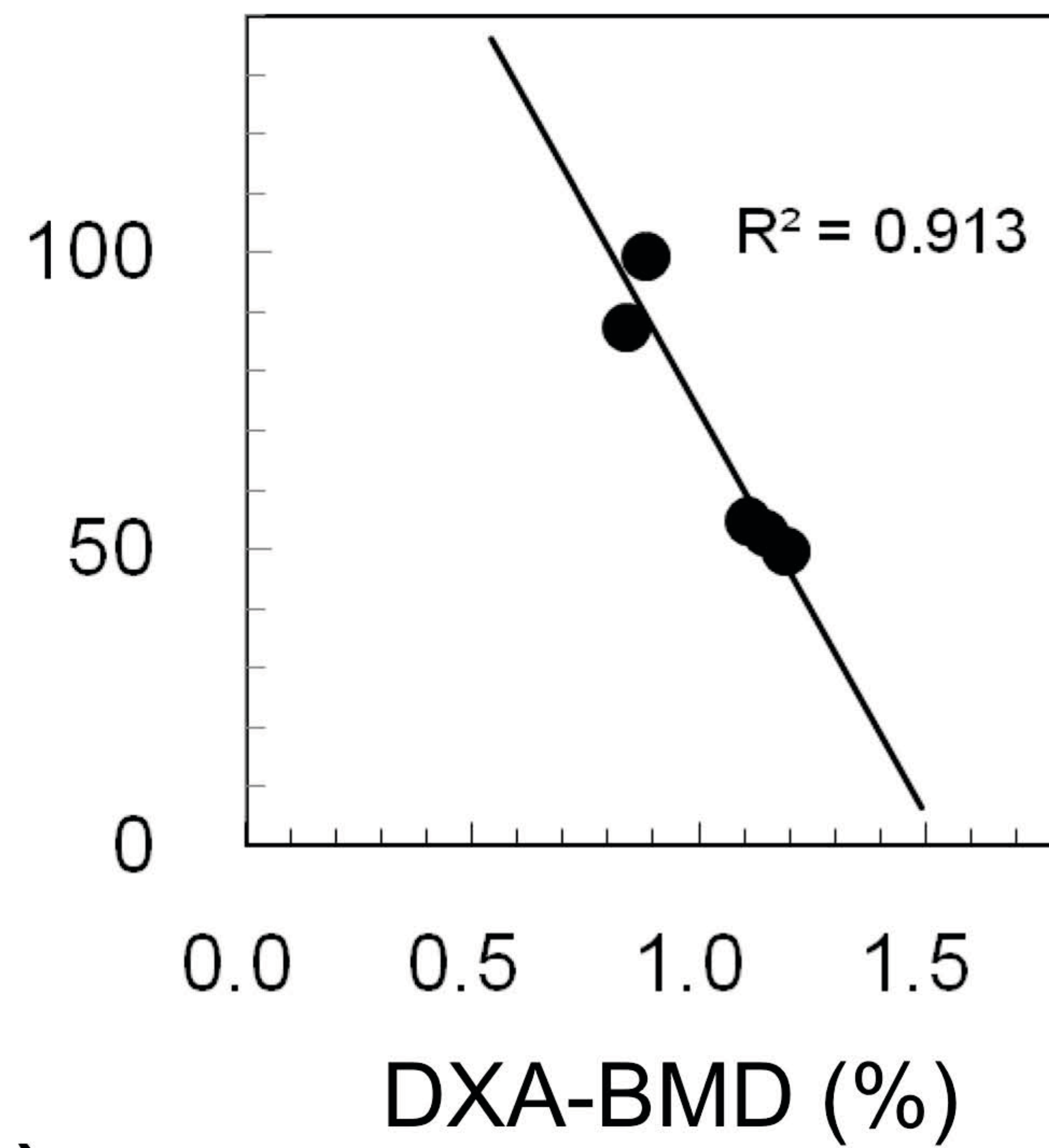


R_2^* of water component (s^{-1})



a)

MRI-derived fat fraction (%)



b)